Title: Graded functional changes in ATL reflect both semantic content and process

Authors: Katya Krieger-Redwood[1], Xiuyi Wang[1,2], Nicholas Souter[1,4], Tirso Rene del Jesus Gonzalez Alam[1], Jonathan Smallwood[2], Rebecca L. Jackson[1], Elizabeth Jefferies[1*]

[1] Department of Psychology, York Neuroimaging Centre, York Biomedical Research Institute, University of York, United Kingdom

[2] CAS Key Laboratory of Behavioral Science, Institute of Psychology, Chinese Academy of Sciences, Beijing, 100101, China

[3] Department of Psychology, Queen's University, Kingston, Ontario, Canada

[4] School of Psychology, University of Sussex, Brighton, United Kingdom

*corresponding author

Abstract

Patients with semantic dementia have degraded conceptual knowledge, accompanied by atrophy of ATL; however, the organisation of ATL is less well-understood, due to signal loss/distortions in ATL in fMRI. We used MBME acquisition and the HCPex-Glasser parcellation to investigate how parcels within ATL respond across different types of semantic content (emotional, contextual, associative, feature) in generative and matching tasks. Areas closer to auditory cortex activated more for associative and emotion-based semantics. An intermediate area nearer to visual cortex was more multi-modal, with equal recruitment across judgments (associative/feature) and generation (emotion/context). The parcel closest to vision activated more for context than emotion. Recruitment was stronger for initial generation than switching to a second association, regardless of content, across ATL parcels. Left ATL activated more than right ATL across content and process (except aSTG). Our results are consistent with the graded-hub-perspective, showing graded transitions from both dorsal and medial ATL towards vATL.

Keywords: Anterior temporal lobe, graded hub, semantic, distance

1. Introduction

The anterior temporal lobes (ATL) are associated with multimodal conceptual representation, but their functional organisation remains controversial. While most researchers now accept that ATL supports aspects of semantic processing, there remains uncertainty about whether site(s) within this broad region support multimodal concepts across categories (Matthew A. Lambon Ralph, Jefferies, Patterson, & Rogers, 2017), or whether there are distinct regions that underpin specific aspects of knowledge pertaining to words, objects, scenes, emotions and people (Hoenig, Sim Ej Fau - Bochev, Bochev V Fau - Herrnberger, Herrnberger B Fau - Kiefer, & Kiefer, 2008; Martin, 2007; Persichetti, Denning, Gotts, & Martin, 2021; Simmons, Martin A Fau - Barsalou, & Barsalou, 2005). ATL is not a unitary system but is composed of multiple anatomical and functional subdivisions which reflect differences in cytoarchitecture, structural and functional connectivity. There is ongoing debate about whether this organisation reflects a patchwork of functions (Persichetti et al., 2021) or whether there is graded functional change within ATL such that subregions of this brain area show systematic functional transitions based on their location (Binney, Hoffman, & Lambon Ralph, 2016; Matthew A. Lambon Ralph et al., 2017; Maya Visser, Jefferies, Embleton, & Lambon Ralph, 2012; M. Visser & Lambon Ralph, 2011). Moreover, the ATL is a largely bilateral system, with both left and right hemispheres contributing to semantic cognition. Much of what we know about the organisation of ATL comes from neuropsychological studies of semantic dementia (characterised by progressive neurodegeneration of anterior and inferior ATL accompanied by degradation of conceptual knowledge) and meta-analyses of neuroimaging studies (Jefferies & Lambon Ralph, 2006; Matthew A. Lambon Ralph, Cipolotti, Manes, & Patterson, 2010; Matthew A. Lambon Ralph, Ehsan, Baker, & Rogers, 2012; Rice, Caswell, Moore, Hoffman, & Lambon Ralph, 2018; Rice, Lambon Ralph, & Hoffman, 2015; M. Visser, Jefferies, & Lambon Ralph, 2009). Both of these methods lack spatial resolution and are therefore not ideal for resolving questions such as which regions in ATL are crucial for aspects of long-term conceptual representation.

A highly influential theory of the role of ATL in semantic cognition is the 'hub and spokes' account, proposed by Patterson and colleagues (2007). This view bridges embodied accounts with 'representational store' accounts of semantic cognition: concepts are formed in a bilateral heteromodal hub system in ATL, which integrates multiple feature types and modalities, including lexical representations, object features like colour, size, shape and motion, actions and valence. This 'hub' allows mapping between different input/output systems i.e., you can name *coffee* from its smell and describe the visual features of an *elephant* from its name. The 'hub' is also able to detect categorical similarity structures that are not easily discernible from a single feature (and/or modality); for example, a *hosepipe* and a *snake* are similar in shape and colour but are found in different locations and are associated with different actions, allowing the semantic system to determine that *hosepipe* is more semantically related to *watering can* (Matthew A. Lambon Ralph, Sage, Jones, & Mayberry, 2010).

Following the original 'hub and spokes' account in 2007, we proposed a graded version of this framework (Matthew A. Lambon Ralph et al., 2017; Rice, Hoffman, & Lambon Ralph, 2015) in which the greatest integration of spoke features emerges in regions of ATL that are maximally distant from unimodal regions, giving rise to high-dimensional multimodal concepts. The macroscale organisation of the temporal lobes reflects two gradients of functional integration, along (i) longitudinal (caudal to rostral) and (ii) lateral axes (STG-ITG and MTG-ITG; Maya Visser et al., 2012). The first of these gradients runs posterior to anterior along the long axis of the temporal lobe, such that relatively posterior parts of the temporal lobe, proximal to visual and auditory cortex, represent modality-specific semantic features, while anterior parts of the temporal lobe provide a store of multimodal semantic information. The second gradient, orthogonal to the posterior to anterior one, runs rostro-caudally with transitions between the superior temporal gyrus (auditory/verbal) and entorhinal/fusiform cortex (visual) respectively, while anatomical subdivisions of ATL that fall between these superior versus medial pathways are more multimodal (Maya Visser et al., 2012; M. Visser & Lambon Ralph, 2011). These patterns of functional change within the temporal lobe are

thought to explain the observation that semantic similarity can be decoded across input modalities and languages in anterior ventrolateral regions (Coutanche & Thompson-Schill, 2014; Murphy et al., 2017). However, it remains somewhat unclear where the multimodal peak of the graded 'hub' is located; an early landmark review described a large swathe of temporal pole as multimodal (Patterson et al., 2007), while multivariate fMRI analyses show decoding of meaning across input modalities in anterior middle and inferior temporal gyrus (but not superior aspects of ATL; Murphy et al., 2017). Recent work has identified common responses to word and picture concepts across functional resonance imaging studies (fMRI) and intracranial electrophysiological recordings in anterior fusiform cortex and inferior temporal gyri (Chen et al., 2016; Rogers et al., 2021).

There is also ongoing debate about the extent to which ATL functions are lateralised. Neuropsychological studies have shown that severe semantic deficits follow bilateral but not unilateral ATL damage: for example, patients with semantic dementia and herpes simplex encephalitis (HSVE) can have very substantial semantic deficits (although the impairment of conceptual knowledge in HSVE shows a more category-specific profile, particularly affecting animals, and the area of brain injury is also more medial than in semantic dementia; Matthew A. Lambon Ralph, Lowe, & Rogers, 2007; Noppeney et al., 2007), while the semantic deficits for patients with unilateral resection for epilepsy are less substantial (M. A. Lambon Ralph, 2014). This has informed the semantic framework suggested by Patterson and others which posit bilateral recruitment of the ATL (M. A. Lambon Ralph, 2014; Patterson et al., 2007; Schapiro, McClelland, Welbourne, Rogers, & Lambon Ralph, 2013). Nevertheless, many researchers have proposed distinctions between left and right ATL in the contributions they make to semantic representation and retrieval; for example, Damasio (2004) proposes that left ATL plays a stronger role in picture naming, as opposed to picture recognition. Other work has suggested that the right ATL might be more important for social semantic retrieval, face recognition and/or emotions (Borghesani et al., 2019; Gainotti, 2015; Irish, Hodges, & Piguet, 2014; I. R. Olson, Plotzker A Fau - Ezzyat, & Ezzyat, 2007; Zahn et al., 2007). However, this suggestion remains controversial, with mixed findings (for reviews see: Ingrid R. Olson,

McCoy, Klobusicky, & Ross, 2013; I. R. Olson et al., 2007; Rice, Lambon Ralph, et al., 2015). A recent study that employed multiple theory of mind and non-social semantic tasks combined with an fMRI protocol optimised for ATL found robust bilateral ventrolateral ATL activation for both social and semantic stimuli, regardless of task type (Balgova, Diveica, Walbrin, & Binney, 2022). Furthermore, a meta-analysis of 97 neuroimaging studies found that activation was predominantly bilateral across task dimensions (e.g., verbal versus non-verbal; social versus non-social; word retrieval versus other tasks; Rice, Lambon Ralph, et al., 2015), suggesting that any hemispheric specialisation is more complex than a simple division in function across left and right ATL.

Lateralisation of semantic cognition within ATL may be further complicated by the requirement to retrieve and manipulate concepts in a controlled way to suit the current goal or context. Activation associated with controlled semantic retrieval – including in inferior frontal gyrus and posterior middle and inferior temporal gyri – is strongly left-lateralised (Rebecca L. Jackson, 2021) and these regions show stronger intrinsic connectivity with each other in the left than the right hemisphere (T. R. J. Gonzalez Alam, Karapanagiotidis, Smallwood, & Jefferies, 2019), suggesting that they form a left-lateralised functional network (T. R. d. J. Gonzalez Alam et al., 2022). This suggests that, in general, semantic control is left-lateralised, while the picture may be more complex for representation regions – where a number of factors may influence laterality. However, ventral ATL is the only site in the semantic network that does not show a lateralised pattern of intrinsic connectivity and task-based activation (T. R. J. Gonzalez Alam et al., 2019; Rebecca L. Jackson, Bajada, Rice, Cloutman, & Lambon Ralph, 2018). Nevertheless, specific regions within ATL could still show left-lateralised responses, reflecting their connectivity with the left-lateralised retrieval network.

Functional magnetic resonance imaging (fMRI) investigations of ATL have been hampered by magnetic susceptibility artefacts caused by the proximity of this brain region to the air-filled sinuses, which produces signal loss and distortions. For this reason, positron emission tomography studies

have often recovered ATL responses in semantic tasks while fMRI studies have not (M. Visser et al., 2009). More recently fMRI sequences designed to recover better signal from ATL have led to an increase in our understanding of this region. These sequences utilise a smaller echo time and/or combine this with multiple echoes; for example, modern multiband multi-echo (MBME) sequences provide better signal-to-noise in ATL (Embleton, Haroon, Morris, Ralph, & Parker, 2010; Halai, Parkes, & Welbourne, 2015; Halai, Welbourne, Embleton, & Parkes, 2014; Poser & Norris, 2007; Poser, Versluis, Hoogduin, & Norris, 2006). Several recent studies using these imaging sequences have examined the functional organisation of ATL in semantic cognition (e.g., Balgova et al., 2022; Binney, Embleton, Jefferies, Parker, & Lambon Ralph, 2010; Binney et al., 2016; Rice, Hoffman, Binney, & Lambon Ralph, 2018; M. Visser, Embleton, Jefferies, Parker, & Ralph, 2010). For example, a key site in the ventral ATL has emerged as multi-modal conceptual integrator due to both its activation profile and structural connectivity – with long range connectivity from primary sensory areas gradually converging on the ventral ATL (Bajada et al., 2017; Rebecca L. Jackson et al., 2018).

In the current research, we examined functional responses within subdivisions of ATL, re-analysing datasets acquired with MBME fMRI to maximise the signal in this region. We focussed on datasets that contrasted different kinds of semantic tasks, to investigate the functional organisation of ATL within the semantic domain. We used the multimodal parcellation of Glasser et al. (2016), projected into volumetric space (Huang, Rolls, Feng, & Lin, 2022), since this parcellation is based on cytoarchitectural and structural features and not only functional connectivity patterns. The first study required participants to generate either emotional states (e.g. *fear* in response to *skydiving*) or meaningful contexts (e.g. *buying something for dinner* in response to *supermarket*) from photographs. The second study examined verbal semantic judgements and asked participants to link words on the basis of either global semantic relationships (e.g. “seaweed – jellyfish”) or specific visual features (e.g. “meatball – moon”). Together, the two studies allowed us to investigate the role of ATL subregions in tasks that require participants to actively generate associations or make decisions about associations presented to them. We examined the effect of semantic content, asking

how regions within ATL differentially respond to emotional versus contextual semantic information, and associative versus feature-based semantic decisions. We also used structural scans from the Human Connectome Project (HCP) to compute the average physical distance along the cortical surface from the vertices in each ATL parcel to structural landmarks denoting the locations of primary visual and auditory cortex. The graded hub account predicts that responses in these tasks will vary topographically in a systematic and gradual fashion. It further anticipates that regions of ATL that are the most equidistant to visual and auditory cortex should show the most 'hub-like' responses – that is, these regions should support semantic cognition irrespective of the content-type being probed or the type of task. We would expect the strongest preferences for particular conditions in the most superior portions of ATL (e.g. anterior superior temporal gyrus, expected to be closest to auditory cortex) and in the most medial regions (e.g. entorhinal cortex, expected to be closest to visual cortex), with gradual functional change across parcels that move towards ventral and lateral regions between these extremes. In particular, recent research predicts a ventral ATL convergence zone, situated a maximum distance from primary sensory-motor cortex and equidistant from visual and auditory input processing regions, allowing it to form fully heteromodal conceptual representations.

2. Method

2.1. Participants

Participants in Studies 1 and 2 were right-handed, between the ages of 18 and 35, with normal or corrected to normal vision, no history of neurological disorder, and no current psychiatric disorder. Participants were students at the University of York, recruited through word of mouth and participant pools, and paid for their time or awarded course credit. Ethical approval for both studies was granted by the York Neuroimaging Centre at the University of York. Informed consent was obtained from all participants prior to participation.

Study 1 (emotion/semantic generation): Thirty-three participants were scanned; with one dataset excluded due to the participant not making associations for the majority (52.1%) of trials. The final sample consisted of 32 participants (24 female; mean age = 20.1, SD = 2.4).

Study 2 (association/feature judgments): Thirty-four adults were scanned; one participant withdrew from the study due to back pain, another participant was withdrawn due to a structural anomaly, and a further participant was unusable due to the participant falling asleep in both scanning sessions. Two further participants were excluded from data analysis due to poor behavioural performance (2SD's below the group mean on the feature matching task). Therefore, the final sample consisted of 29 participants (24 female; mean age = 21.1, SD = 3.1). Another 30 native English speakers, who did not take part in the main fMRI experiment, rated the colour and shape similarity and semantic association strength for each word pair (21 females; age range: 18 – 24 years).

We also used structural MRI scans from the HCP dataset to examine distance of each ATL parcel from auditory and visual primary landmarks along the cortical surface. Informed consent was obtained, and the study was approved by the Institutional Review Board of Washington University at St. Louis. We used the R1096 group from the HCP S1200 project, containing structural scans for 1096 participants (https://balsa.wustl.edu/wN6Zv; Glasser et al., 2016).

2.2. Tasks and Paradigms

2.2.1. Study 1: Emotion and Context Generation and Switch

This study required participants to generate context or emotion associations to pictures, and then retrieve a new association to the same picture in a second phase. Stimuli were taken from the International Affective Picture System (IAPS; Lang, Brady, & Cuthbert, 2008), a database of pictures normed for valence and arousal. Thirty-six pictures were selected for *emotion* associations and were either positive (valence mean > 6) or negative (valence mean < 4), with an equal number of positive

and negative images in each experimental run. A further thirty-six pictures were selected for *context* associations, all of neutral valence (mean valence between 4 and 6). Valence for pictures across conditions was significantly different (negative emotion < *context* < positive *emotion* pictures; U < 1, $p < .001$). Ratings of mean arousal were significantly higher for *emotion* than *context* pictures (U = 221.0, $p < .001$), but were matched between positive and negative *emotion* images (U = 153.5, $p = .791$). Identifiers for each image and normed ratings of valence and arousal are provided in Supplementary Table S1.

Trials were presented in mini-blocks of association type (emotion/context) with six trials in each mini-block per run. The order of trials within a run was consistent across participants, but run order was counterbalanced across participants. Each mini-block started with a 2 second instruction (i.e., 'SEMANTIC' or 'EMOTION'), and each trial started with a jittered fixation cross (1-3 s). During the 'GENERATE' phase participants were presented with a picture; during *context* associations, participants identified a meaningful context from their general knowledge (i.e., they were asked not to rely on a specific episodic memory), and for emotion associations, participants were asked to embody emotions evoked by the image when generating the association. The 'SWITCH' phase required participants to stop reflecting on their initial association, and generate a new one. The same image was used in both generate and switch phases of the trial. Trial time across *generate* and *switch* phases was jittered between 3.5 and 6.5s, with an average of 5s. After each *generate* and *switch* phase, participants rated the strength of their self-generated association on a scale from 1 (no real relationship) to 7 (very strong relationship). A final rating of switch difficulty (i.e., how difficult it was to switch from initial association to a new one) was given at the end of the whole trial on a scale from 1 (very easy) to 7 (very difficult). Each rating period lasted 3s (Figure 2; detailed task schematic in supplementary materials Figure S1).

Immediately following the scan, participants completed a 'recall' assessment. Pictures were presented in the same order as in the scanner, and participants typed the contexts or emotions they

generated, as well as rating confidence in recall (from 1-7), for both the *generate* and *switch* phases. This data was used to qualitatively validate that participants performed the task as intended.

2.2.2. Study 2: Association and Feature Judgments

In the feature matching task, participants made yes/no decisions about whether two visually presented words shared a particular visual feature (colour or shape; Figure 3). The trials were created such that participants would respond yes to roughly half of the trials, allowing us to separate the neural response to yes and no decisions. For example, for colour matching: participants would respond 'yes' to "DALMATIAN – COW", due to their colour similarity, but 'no' to "COAL -TOOTH" due to the lack of colour feature similarity. The task was split into four runs, with two feature conditions (colour/shape), presented in a mixed design. The feature type was split into four mini blocks (2mins 30s each), resulting in a total run time of 10.55mins. In each mini block, 20 trials were presented in a rapid event-related design. In order to maximize the statistical power, the stimuli were presented with a temporal jitter randomized from trial to trial (Dale, 1999), with a variable inter-trial of 3 to 5 s. Each trial started with a fixation, followed by the feature type (colour/shape) at the top of the screen, and the concepts presented centrally (Figure 3, detailed task schematic in supplementary materials Figure S1). These remained on-screen until the participant responded, or for a maximum of 3 s. The condition order was counterbalanced across runs and run order was counterbalanced across participants.

In the association task, participants made yes/no decisions about whether two visually presented words shared a semantic association or not. The trials were created such that participants would respond yes to roughly half of the trials, allowing us to separate the neural response to yes and no decisions. The same stimuli were used across both semantic feature matching and semantic associations task. For example, "DALMATIAN – COW' are semantically related (and also have similar colour) whereas "COAL – PUMA" are not semantically related (but still share the colour feature). This task was split into four runs, presented in a rapid event-related design. Each run consisted of 80

trials (10.35 mins per run), and the procedure was the same as the feature matching task except only two words were presented on the screen (as no condition cue was needed).

Half of the participants responded with their right index finger to indicate yes and with their middle finger to indicate no; the other half pressed the opposite buttons. The feature and association task sessions were separated by one week, and their order was counterbalanced across participants.

For both Studies 1 and 2, participants completed practice sessions the day before their scanning session via Zoom. Python scripts used for presentation of the semantic tasks are available on Open Science Framework (OSF; Study 1 at https://osf.io/498ur/ and Study 2 at https://osf.io/p2s3w/?view_only=c61215613db24343ad28a51f26744ab8).

2.3 Parcel Selection

Glasser et al.'s (2016) parcellation was used to define subdivisions of the ATL as it takes both functional and structural architecture into account, and allows us to compare left and right hemispheres easily. We used the HCPex version (Huang et al., 2022) of the Glasser parcellation: this is in volumetric space, allowing us to interrogate our functional MRI data using FSL. We selected ROIs with cortex labels "lateral temporal" and "medial temporal" and also included one parcel from "auditory association" cortex, to include anterior STG, in order to cover the anterior half of the temporal lobe. Therefore, the following parcels were selected: STGa, Entorhinal Cortex (EC), Perirhinal Ectorhinal Cortex (PeEc), TE1 anterior (TE1a), TG dorsal (TGd), and TG ventral (TGv). A table including the Glasser labels and HCPex labels for these regions is included in Supplementary Materials (Table S2).

2.4. Image Acquisition

HCP dataset: MRI acquisition protocols of the HCP dataset have been described previously (Barch et al., 2013; Glasser et al., 2013). Images were acquired using a customized 3T Siemens Connectome scanner with a 100 mT/m SC72 gradient set and using a standard Siemens 32-channel radiofrequency receive head coil. Participants underwent the following scans: structural (at least one T1-weighted (T1w) MPRAGE and one 3D T2-weighted (T2w) SPACE scan at 0.7-mm isotropic resolution), rsfMRI (4 runs ×14 min and 33 s), and task fMRI (7 tasks, 46.6 min in total).

Semantic Datasets: Whole brain structural and functional MRI data were acquired using a 3T Siemens MRI scanner utilising a 64-channel head coil, tuned to 123 MHz at the York Neuroimaging Centre, University of York. We used a multiband-multiecho (MBME) EPI sequence with the following parameters: TR=1.5 s; TEs = 12, 24.83, 37.66 ms; 48 interleaved slices per volume with slice thickness of 3 mm (no slice gap); FoV = 24 cm (resolution matrix = 3x3x3; 80x80); 75° flip angle; volumes per run below; 7/8 partial Fourier encoding and GRAPPA (acceleration factor = 3, 36 ref. lines; multi-band acceleration factor = 2). Structural T1-weighted images were acquired using an MPRAGE sequence (TR = 2.3 s, TE = 2.26 s; voxel size = 1x1x1 isotropic; 176 slices; flip angle = 8°; FoV= 256 mm; interleaved slice ordering). The number of runs, run time and volumes collected per run are as follows: emotion/context task = 6 runs x 4.5 mins (180 volumes); feature task = 4 runs x 10.55 mins (422 volumes); association task = 4 runs x 10.35 (414 volumes).

For the association/feature study, we also collected a high-resolution T2-weighted (T2w) scan using an echo-planar imaging sequence (TR = 3.2 s, TE = 56 ms, flip angle = 120°; 176 slices, voxel size = 1x1x1 isotropic; Fov = 256 mm), and a 9 minute resting-state scan (acquired using an EPI sequence; 80° flip angle; GRAPPA acceleration factor of 2; resolution matrix = 3x3x4; 64x64; TR = 3s, TE = 15 ms, FoV = 192 mm) that were not used in the current project.

2.5. Image Pre-processing

HCP dataset: We used HCP's minimal pre-processing pipelines (Glasser et al., 2013). Briefly, for each subject, structural images (T1w and T2w) were corrected for spatial distortions. FreeSurfer v5.3 was used for accurate extraction of cortical surfaces and segmentation of subcortical structures (Dale, 1999; Fischl, Sereno, & Dale, 1999). To align subcortical structures across subjects, structural images were registered using non-linear volume registration to the Montreal Neurological Institute (MNI152) space. Subcortical data were also projected to the set of extracted subcortical structure voxels and combined with the surface data to form the standard CIFTI grayordinate space. Data were smoothed by a 2-mm FWHM kernel in the grayordinates space that avoids mixing data across gyral banks for surface data and avoids mixing areal borders for subcortical data. For accurate cross-subject registration of cortical surfaces, a multimodal surface matching (MSM) algorithm (Robinson et al., 2014) was used to optimize the alignment of cortical areas based on features from different modalities. MSMSulc ("sulc": cortical folds average convexity) was used to initialize MSMAll, which then utilized myelin, resting-state network, and rfMRI visuotopic maps.

Semantic tasks: A MBME sequence was used to optimise signal from the anterior and medial temporal regions, while maintaining optimal signal across the whole brain (Halai et al., 2014). We used TE Dependent ANAlysis (tedana; version 0.0.12; Prantik Kundu et al., 2013; The tedana Community et al., 2021; P. Kundu, Inati Sj Fau - Evans, Evans Jw Fau - Luh, Luh Wm Fau - Bandettini, & Bandettini, 2012) to combine the images. Anatomical pre-processing (fsl_anat; https://fsl.fmrib.ox.ac.uk/fsl/fslwiki/fsl_anat) included re-orientation to standard MNI space (fslreorient2std), automatic cropping (robustfov), bias-field correction (RF/B1 – inhomogeneity-correction, using FAST), linear and non-linear registration to standard-space (using FLIRT and FNIRT), brain extraction (using FNIRT, BET), tissue-type segmentation (using FAST) and subcortical structure segmentation (FAST). The multi-echo data were pre-processed using AFNI (https://afni.nimh.nih.gov/), including de-spiking (3dDespike), slice timing correction (3dTshift;

heptic interpolation), and motion correction (3dvolreg applied to echo 1 to realign all images to the first volume; these transformation parameters were then applied to echoes 2 and 3; cubic interpolation). Runs with motion greater than 1.1mm (absolute) were excluded from analyses across both semantic studies. This resulted in the removal of the final run for two participants for the feature matching task and for one participant for the association task. Relative displacement was less than .18mm across both Studies 1 and 2.

2.6. Cortical Geometry - Global Minimum distance to Primary Sensory-motor Landmarks

We asked whether the physical proximity to primary sensory-motor regions (i.e., spokes) might influence the function of ATL regions. We investigated this issue by calculating the geodesic distance between each ATL parcel and key landmarks associated with primary visual, auditory and somatomotor cortex. We used these values to identify the minimum geodesic distance to each primary sensory-motor region for each ATL parcel. The following three landmarks were used (i) central sulcus (primary somatosensory/motor cortex), (ii) temporal transverse sulcus (primary auditory cortex), and (iii) calcarine sulcus (primary visual cortex). Since cortical folding patterns vary across participants, and individual variability in cortical folding increases with cortical surface area, both the shapes of these landmarks and the number of vertices within each landmark might show individual variability (Van Essen et al., 2019). We used participant-specific landmark label files to locate the participant-specific vertices belonging to each landmark and participant-specific parcellation to locate the vertices within each parcel (Wang et al., 2023).

Geodesic distance along the “midthickness” of the cortical surface (halfway between the pial and white matter) was calculated using the Connectome Workbench software with an algorithm that measures the shortest path between two vertices on a triangular surface mesh (Mitchell, Mount, & Papadimitriou, 1987; O'Rourke, 1999). This method returns distance values that are independent of mesh density. Geodesic distance was extracted from surface geometry (GIFTI) files, following surface-based registration (Robinson et al., 2014). To ensure that the shortest paths would

only pass through the cortex, vertices representing the medial wall were removed from the triangular mesh in this analysis.

We calculated the minimum geodesic distance between each vertex and each landmark. Specifically, for the landmark central sulcus, we calculated the geodesic distance between vertex *i* outside central sulcus and each vertex within the central sulcus (defined for each individual; see above). We then found vertex *j* within the central sulcus closest to vertex *i*, and extracted this value as the minimum geodesic distance between vertex *i* and this landmark. To compute the minimum geodesic distance between parcel *k* and the central sulcus, we computed the average minimum distance across all the grayordinate vertices in parcel *k* to the vertices within the central sulcus. We used the same procedure to calculate minimum geodesic distance between each parcel and all three sensory-motor landmarks (calcarine and temporal transverse sulci as well as central sulcus).

2.7. fMRI Data Analysis

Individual level analyses were conducted using FSL-FEAT version 6 (FMRIB's Software Library, www.fmrib.ox.ac.uk/fsl; Jenkinson, Bannister, Brady, & Smith, 2002; Smith et al., 2004; Woolrich et al., 2009). Denoised optimally-combined time series output from tedana were submitted to FSL and pre-processing included high-pass temporal filtering (Gaussian-weighted least-squares straight line fitting, with sigma = 50s), linear co-registration to the corresponding T1-weighted image and to MNI152 standard space (Jenkinson & Smith, 2001), spatial smoothing using a Gaussian kernel with full-width-half-maximum of 6 mm, and grand-mean intensity normalisation of the entire 4D dataset by a single multiplicative factor. Pre-processed time series data were modelled using a general linear model correcting for local autocorrelation (Woolrich, Ripley, Brady, & Smith, 2001). No motion parameters were included in the models, as the data had already been denoised as part of the TEDANA pipeline (P. Kundu et al., 2012).

Study 1 examined emotion and context across generation and switch phases. EVs were as follows: (1) context generate, (2) context switch, (3) emotion generate, (4) emotion switch, (5) all self-report rating periods and (6) condition prompt from the start of each mini-block, (7) parametric context switch difficulty, (8) parametric emotion switch difficulty. These parametric EVs are not relevant to the current study; ANOVA's containing these variables can be found in Supplementary Materials (Table S4).

Study 2 examined association and feature judgments. EVs were as follows: (1) the mean activity to yes responses, (2) mean for no responses, (3) parametric effects for yes responses, (4) parametric effects for no responses. Parametric regressors were derived from an independent set of participants (see Participants). For the association task, we included rated association strength for each word pair on a five-point scale (1 = not at all related to 5 = very related). For the feature matching task, we examined rated feature similarity of the pair of items (1 = not similar at all to 5 = very similar). These parametric EVs are not relevant to the current study; ANOVAs containing these variables can be found in Supplementary Materials (Table S6). A fifth EV captured any incorrect (feature matching) or missed (association/feature) trials. Response type (yes/no) was entered into all ANOVAs for Study 2, however it did not significantly interact with parcel (see Supplementary Materials, Tables S5 and S6).

We extracted percent signal change for each ATL parcel from the main EVs in Studies 1 and 2. Additional EVs (e.g., parametric) are described in Supplementary Materials (Tables S4 and S6).

3. Results

3.1. Distance of ATL Parcels to Primary 'Spoke' Regions

We asked whether parcels in ATL show different spatial proximity to sensory-motor spoke regions (i.e., somatomotor, auditory and visual). Geodesic distance values from the six ATL parcels and three primary landmarks (for each hemisphere) were examined in an omnibus ANOVA

(hemisphere (2) x landmark (3) x parcel (6); Figure 1; Figure S2). The data for each parcel are identified using a colour key. There was a significant three-way interaction ($F(5,5408)=445.7$, $p < .001$); the motor landmark was further than the auditory and visual landmarks for all the ATL parcels. ANOVAs specifically comparing auditory and visual landmarks (given earlier research showing a graded hub architecture across verbal/picture and auditory/visual tasks; Rice, Hoffman, et al., 2015; Maya Visser et al., 2012) revealed that anterior superior and middle temporal regions (STGa shown in red, TE1a shown in cyan, and TGd shown in mint) sit closest to auditory cortex ($F(1, 1095) > 37107$, $p < .001$), while parcels in medial and ITG regions (PeEC shown in blue, EC shown in green) sit closest to vision ($F(1, 1095) > 33949$, $p < .001$). The TG ventral ATL parcel (shown in yellow) was the most equidistant to auditory and visual cortices (although still significantly closer to vision; $F(1, 1095) = 785.8$, $p < .001$). This proximity of ATL parcels to auditory and visual spoke regions may give rise to differential responses across tasks depending on the degree to which they rely on processes that tap auditory versus visual conceptual retrieval.

3.2. Overlaps Between ATL Parcels and Intrinsic Connectivity Networks

Next, we examined the overlap of the ATL parcels with the Yeo 17 network parcellation (Yeo et al., 2011) to establish which resting-state networks these regions of ATL sit within. These overlaps are shown in the pie charts on the right-hand side of Figure 1. Parcel identity is indicated by the colour of the outline of each pie chart (see footnote of Figure 1 for parcel names). STGa (in red) showed the greatest overlap with auditory and lateral DMN networks. TE1a (in MTG, shown in cyan) and TGd (in temporal pole, shown in mint) largely fell within the limbic-A network. TGv (in anterior ITG/fusiform, shown in yellow) showed the greatest overlap with lateral and core DMN. PeEC (in fusiform cortex, shown in blue) showed overlap with Limbic-A and lateral DMN. Finally, EC (in parahippocampal gyrus, shown in green) largely fell within the limbic-A network. Most regions were similar across left and right hemisphere in terms of Yeo 17 network assignment. However, the TGv

ATL site showed a pronounced difference between hemispheres – from lateral DMN (purported to be more semantic) in the left hemisphere to core DMN in the right.

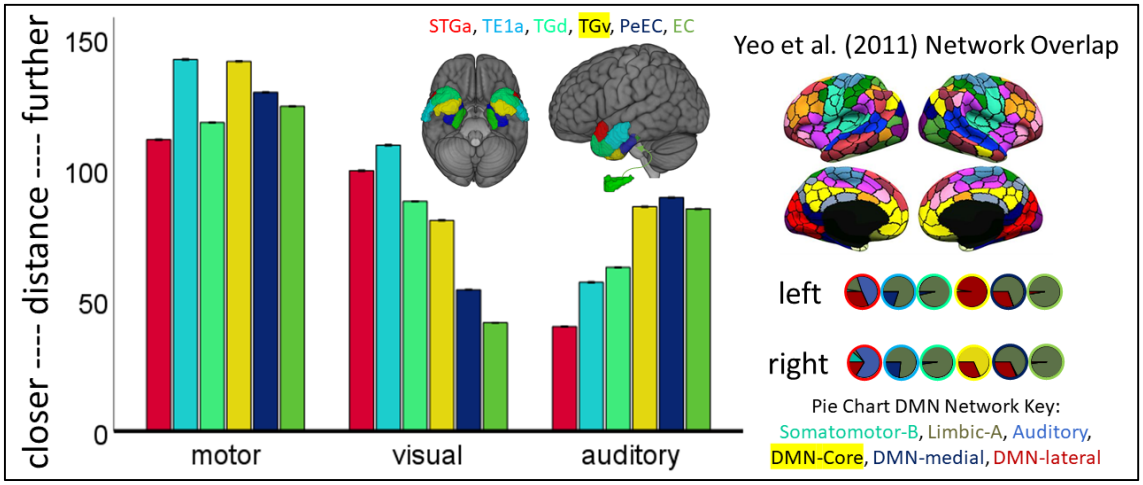

Figure 1. ATL parcel distance to primary landmarks. Left-hand bar chart: Distance of ATL parcels to primary sensory-motor regions (motor, visual and auditory). Bars show estimated marginal means, and 95% confidence intervals, of minimum distance, averaged across all the vertices in each ATL parcel. Smaller numbers = closer proximity. The parcels are colour-coded and presented in the following order from left to right: Red = STGa; Cyan = TE1a (MTG); Mint = TGd (temporal pole); Yellow = TGv (aITG/fusiform); Dark blue = PeEc (fusiform); Green = EC (parahippocampal). Right-hand pie charts: Overlap with functional networks defined by Yeo et al. (2011). These networks are shown on the brain images, and the pie chart wedges use corresponding colours. Each small pie chart refers to the network overlaps for a specific ATL parcel, with the left and right hemispheres shown separately. The outline of each pie chart indicates which parcel is displayed, using the same colour code as the bar chart displaying cortical distance data.

3.3. Activation in Study 1: Emotion and Context Generation and Switch

An omnibus ANOVA confirmed interactions between parcel and semantic content (emotion versus context; $F(2.9, 91.4) = 23.355$, $p < .001$) as well as between parcel and task phase (generate versus switch; $F(3, 99) = 10.4$, $p < .001$); Supplementary Table S3). The results are shown in Figure 2.

The regions partially overlapping with STG (STGa and TGd), which were closest to auditory cortex, showed stronger activation for emotional associations than contexts ($F(1, 31) > 26$, $p < .001$). TE1a within MTG, which was also closer to auditory than visual landmarks, *deactivated* equally for both conditions (as well as for switch and generate; $F(1, 31) < 1$). TGv, which is more equidistant between visual and auditory regions, also activated more strongly for the emotion condition ($F(1, 31) = 16.6$, $p < .001$). In contrast, one of the regions closer to vision (EC) activated more for the context associations ($F(1, 31) = 5.9$, $p = .02$), while PeEC showed no difference for content type.

The ATL regions also showed different responses to task phase (generate versus switch). Activation was stronger for generate than switch conditions in STGa, TGv ($F(1, 31) > 8$, $p \leq .008$) and both regions closer to vision (PeEc and EC; $F(1, 31) > 17$, $p < .001$) suggesting that many ATL regions respond more strongly to the retrieval requirements of initial generation than the control demands involved in switching to a new association. However, the response to generate and switch was equivalent in MTG and temporal pole sites, TE1a and TGd, within the limbic network.

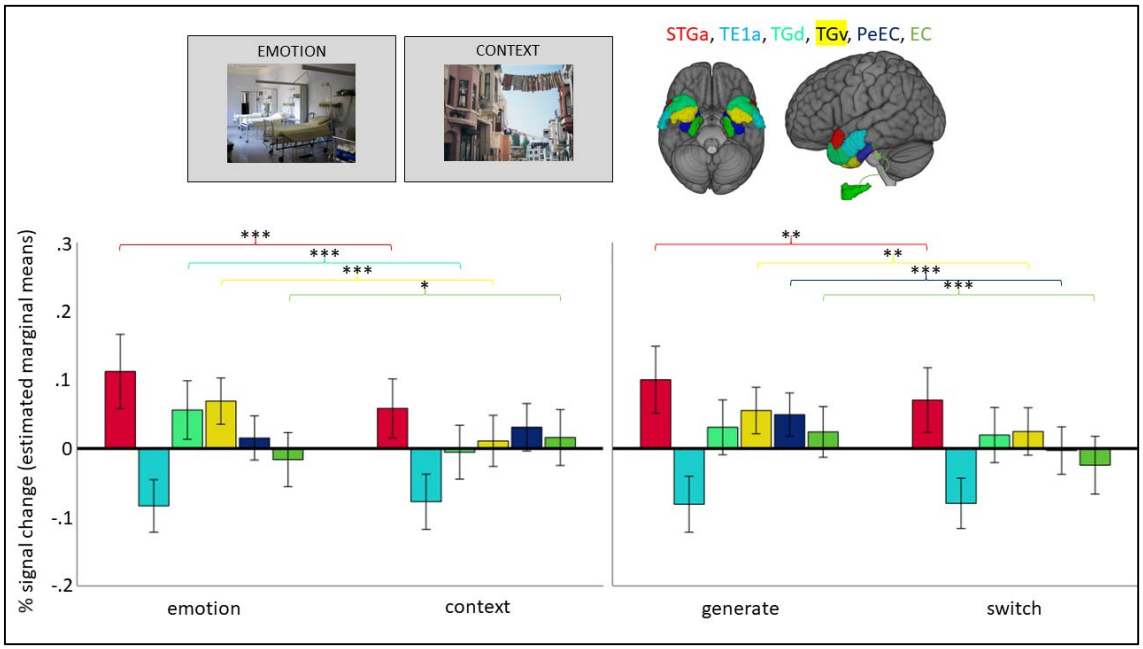

Figure 2. Results from Study 1. Top left: Emotion/Context picture examples. Bottom left: interactions of parcel and emotion/context conditions; bottom right interactions of parcel and generate/switch. Bars show estimated marginal means, and 95% confidence intervals. The parcels are colour-coded and presented in the following order from left to right: Red = STGa; Cyan = TE1a (MTG); Mint = TGd (temporal pole); Yellow = TGv (alTG/fusiform); Dark blue = PeEc (fusiform); Green = EC (parahippocampal). These colours match the brain view and colour key in the top right of the figure. *$p < .05$, **$p < .01$, **$p \leq .001$.

3.4. Activation in Study 2: Association and Feature Judgments

An omnibus ANOVA confirmed that regions of ATL are differentially sensitive to associative versus feature matching ($F(2.9, 81) = 2.7$, $p = .05$; Supplementary Table S5). Superior and middle temporal regions closest to auditory cortex showed more activation (STGa) or less deactivation (TE1a and TGd) for associative than feature decisions ($F(1, 28) > 6$, $p < .02$). Regions that were closer to visual cortex responded equivalently to the two decision types (TGv: $F(1, 28) < 1$; PeEc: $F(1, 28) = 3$, $p = .09$; EC: $F(1, 28) = 3.5$, $p = .07$). This suggests that ATL regions closer to auditory landmarks are

more relevant to the retrieval of global semantic associations than to decisions about specific visual features, while ATL regions that sit at an intermediate (e.g., TGv) position and those closer to visual cortex are engaged equally by both tasks (Figure 3).

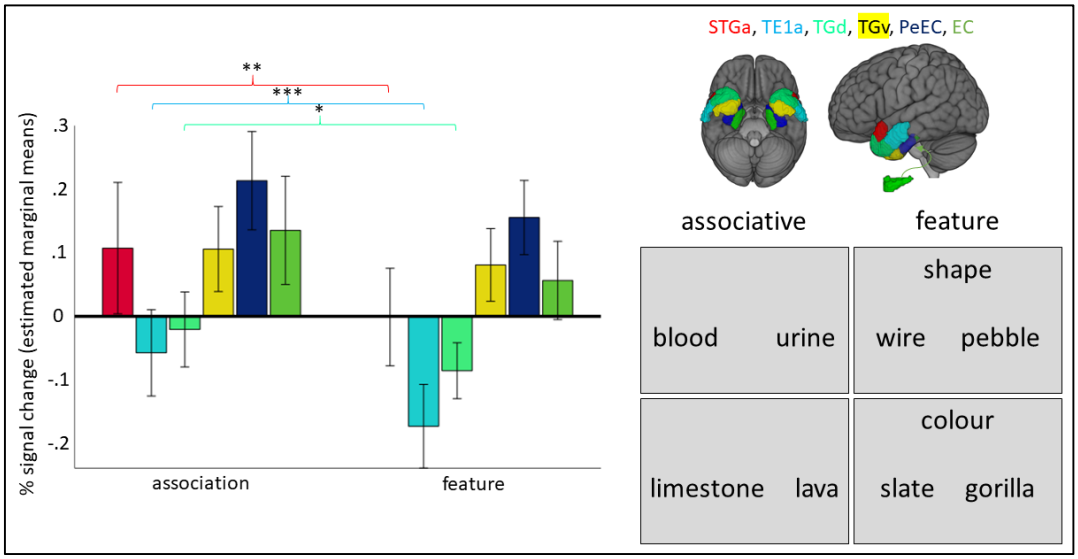

Figure 3. Results from Study 2. Left: interactions of parcel and association/feature conditions. Bars show estimated marginal means, and 95% confidence intervals. The parcels are colour-coded and presented in the following order from left to right: Red = STGa; Cyan = TE1a (MTG); Mint = TGd (temporal pole); Yellow = TGv (aITG/fusiform); Dark blue = PeEc (fusiform); Green = EC (parahippocampal). These colours match the brain view and colour key in the top right of the figure. Bottom right: Feature matching (by colour and shape) and global semantic association examples. *$p < .05$, **$p < .01$, **$p \leq .001$.

3.5. Hemispheric Differences

Both omnibus ANOVAs revealed parcel by hemisphere interactions ($F(3, 81\text{-}89) > 6$, $p < .001$), suggesting that the engagement of ATL regions varied across hemispheres depending on the

task. For Study 1 which required the generation of a response from a pictured input (regardless of emotion versus context and initial generation versus switch), areas closer to auditory cortex showed differential activation between left and right hemispheres: STGa and TGd activated more in the left hemisphere than the right hemisphere, while TE1a was deactivated more in the right hemisphere than the left hemisphere ($F(1, 31) > 11$, $p \leq .002$). Ventral ATL (TGv) was also more strongly activated in the left than right hemisphere for these generative conditions ($F(1, 31) = 6$, $p < .02$). The two areas closest to visual cortex were not differentially activated across hemispheres in Study 1 ($F(1, 31) < 1$).

For Study 2 which required semantic judgments about written words (rather than the generation of associations and/or contexts), areas closer to vision (PeEc, EC) were significantly more active in the left than the right hemisphere ($F(1, 28) > 10$, $p \leq .003$). In contrast, STGa which is closer to auditory cortex, was more active in the right hemisphere ($F(1, 28) = 5$, $p = .04$), while TE1a was more strongly *deactivated* in the right hemisphere ($F(1, 28) = 6$, $p = .02$). Ventral ATL (TGv) was recruited equivalently across hemispheres ($F(1, 28) < 1$). This suggests that hemispheric differences in ATL function vary across subregions in a task-dependent fashion. When generating semantic information, there is strong left-lateralisation in parcels closer to auditory cortex, while judgments about semantic stimuli elicit a lateralised response in regions closer to vision, with an intermediate region responding the same across hemispheres when making judgments.

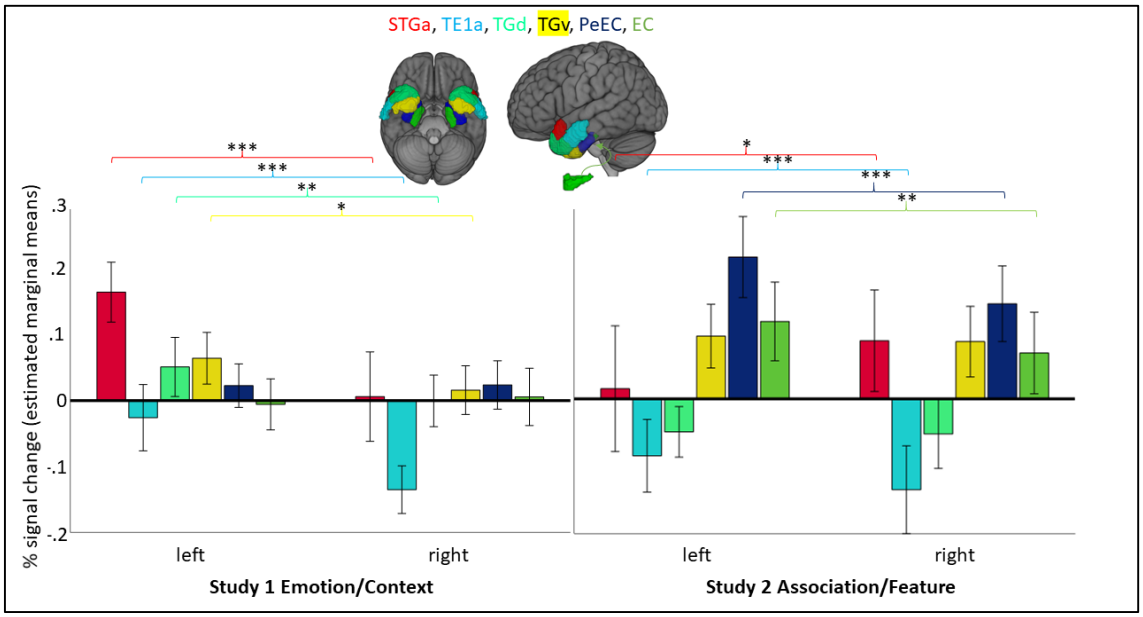

Figure 4. Effects of Hemisphere in Studies 1 and 2. Differential recruitment of parcels across hemispheres for context/emotion generation (initial and switch) and feature/association judgments. Bottom left interactions of parcel and emotion/context and association/feature (bottom right). Bars show estimated marginal means, and 95% confidence intervals. The parcels are colour-coded and presented in the following order from left to right: Red = STGa; Cyan = TE1a (MTG); Mint = TGd (temporal pole); Yellow = TGv (aITG/fusiform); Dark blue = PeEc (fusiform); Green = EC (parahippocampal). *$p < .05$, **$p < .01$, **$p \leq .001$.

4. Discussion

While there are relative differences in activation based on different feature types/categories, our work suggests that, at the macroscale, there are systematic functional transitions within ATL reflecting a superior to medial gradient, consistent with the 'graded hub' hypothesis. Functional differences between superior and medial portions of ATL were observed across two studies that used contrasting inputs, responses and types of concept, suggesting that this superior to medial gradient reflects a fundamental property of ATL organisation. These functional changes were also mirrored by the physical distances from ATL parcels to primary sensory-motor

landmarks along the cortical surface: superior regions of ATL are closer to auditory cortex, and medial regions are closer to visual cortex, with the most equidistant region between auditory and visual cortex found in a ventral ATL parcel, TGv. In Study 1, we found that ATL regions closer to auditory cortex responded more strongly to the generation of emotional responses, including anterior ITG (TGv), while the ATL parcel closest to vision responded more strongly during the generation of meaningful contexts. Study 2 showed that associative judgments activated ATL regions closer to auditory cortex more than feature judgments. In contrast, anterior ITG (TGv) and ATL regions closer to vision were equivalently active across associative and feature judgments. Finally, we explored hemispheric differences. Left and right ATL regions were not differentially sensitive to the content of the task (i.e., emotion, context, association, feature), but nevertheless, hemispheric differences in ATL function varied across subregions in a task-dependent fashion. Left hemisphere parcels closer to auditory cortex were more responsive to the generative tasks in Study 1, regardless of the content (i.e., emotion versus context), while left hemisphere parcels closer to visual cortex were more responsive to the matching tasks in Study 2 – again irrespective of the task demands (association versus feature matching). Taken together, these results suggest that there is sensitivity within ATL to semantic task content that varies across parcels in an orderly fashion.

These findings are summarised in Figure 5. ATL parcels closer to auditory cortex (shown in warmer colours) were more responsive to tasks requiring emotional associations for a stimulus (as opposed to contexts), and showed stronger activation to global semantic associations (as opposed to feature-based judgments). These regions closer to audition also demonstrated more left-lateralised responses in the semantic generation task. Whilst there were very few examples of right-lateralised responses in ATL, STGa did show a stronger response to feature matching in the right than left-hemisphere. This lateralisation within more auditory parts of ATL may reflect an influence left-lateralised language processing: generation tasks and global association matching might be more dependent on language, while visual feature matching might be a semantic task that is less dependent on language.

ATL regions were not sensitive to manipulations of difficulty or the decision type (i.e., yes or no). This might reflect the ATL's key position as a representational hub, with other regions (e.g., the semantic control and multiple demand networks) acting upon this hub to guide retrieval in a context appropriate and goal-driven manner (Duncan, 2010; Fedorenko, Duncan, & Kanwisher, 2013; Rebecca L. Jackson, 2021). This is consistent with neuropsychological evidence, as the deficits in patients with semantic dementia (with progressive atrophy centred on ATL) appear to reflect the degradation of concepts, with poor performance even when control demands are low. In contrast, semantic aphasia patients (with intact ATL, but damaged control systems) are sensitive to task demands, but can successfully identify concepts when the need for control is minimised (Jefferies & Lambon Ralph, 2006).

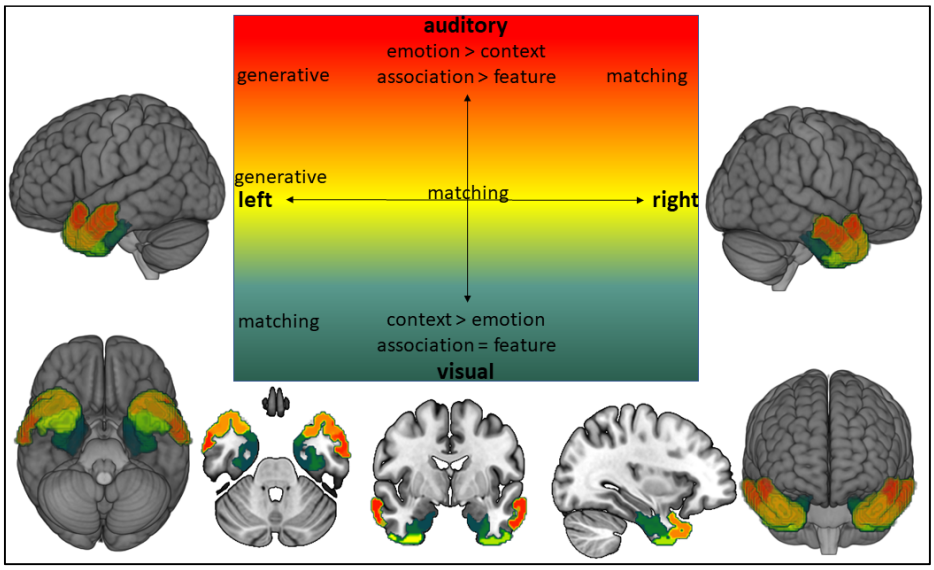

Figure 5. Descriptive summary of results. Summary of the results of this study, with maps of relative distance from auditory and visual areas. Warmer colours represent closer distance to auditory cortex, while darker green colours represent greater proximity to vision. Yellower colours denote regions that fall between vision and audition. The coloured text box highlights how this dimension is associated with functional change and lateralisation in Studies 1 and 2. The vertical dimension shows functional change associated with auditory to visual proximity. The horizontal dimension indicates how the lateralisation of the response varies across tasks in different ATL regions.

Our study helps to delineate relative differences, using parcels placed within the larger convergence zone of the ATL, in activation for different types of semantic content (i.e., associative, contextual, featural, emotional). These relative differences in engagement converge on two key sites: TGv and PeEc. Both of these sites demonstrated a more uniform response across content type in studies 1 and 2, and have, in previous research, been shown to have the highest volume loss in semantic dementia and maximal activation in fMRI for semantic judgments (Binney et al., 2010), leading the authors to identify these two regions as the candidate representational 'hub'. The TGv site sits within the ventral anterior ATL (e.g., anterior ITG) and was the most equidistant between visual and auditory cortex; therefore, it has an appropriate topographical location for the centre of the heteromodal semantic convergence zone. We did not directly test semantic activation in response to auditory and visual inputs but TGv showed a stronger response to the generation of emotions than contexts (like sites towards auditory cortex) and a common and equal response across global association and feature matching decisions (like sites towards visual cortex). In this way, it showed a functional profile that was intermediate between superior and medial ATL. Despite overlapping with different DMN networks in the left and right hemisphere, the TGv site did not show blanket deactivation to semantic tasks. Even in the right hemisphere, where this site overlapped with core DMN, semantic judgements elicited activation (nevertheless, for the generation task, right TGv was less engaged than its left homologue, which sits predominantly in the lateral DMN). This is in line with previous research showing that parts of the ATL that sit with in the DMN activate for semantic tasks (regardless of stimulus modality), but deactivate for non-semantic tasks in line with the general DMN (Humphreys, Hoffman, Visser, Binney, & Lambon Ralph, 2015). In summary, TGv sits in the DMN and showed positive activation particularly across semantic tasks.

The second site with a relatively heteromodal response was PeEc (in the fusiform) and this site overlaps with the co-ordinates previously reported in studies of semantic cognition identifying

this region as a strong candidate for the heteromodal convergence zone (Binney et al., 2010; T. R. J. Gonzalez Alam et al., 2019; Rebecca L. Jackson, Hoffman, Pobric, & Lambon Ralph, 2015; R. L. Jackson, Hoffman, Pobric, & Lambon Ralph, 2016). For example, these previous studies demonstrated that this site was equivalently active for decisions about conceptual association (e.g., dog – bone) and conceptual similarity (e.g., dog – wolf; Rebecca L. Jackson et al., 2015) and does not show a lateralised pattern of intrinsic connectivity and task-based activation (T. R. J. Gonzalez Alam et al., 2019; R. L. Jackson et al., 2016). Our data are consistent with these observations, as ventromedial aspects of ATL (i.e., PeEc) showed the strongest response during semantic judgements to written words and this response was equal across semantic associations and feature judgements, in line with the view that this area supports the retrieval of different kinds of semantic relations. We also found that this site does not show the equidistance from visual and auditory cortex that might be expected of a semantic convergence zone according to the gradient hub account. In summary, it seems likely - from our results - that multiple ATL sites differentially contribute to different aspects of semantic cognition, even though there are gradual changes in the functional profile across ATL parcels from superior through ventrolateral regions to medial ATL.

This profile is different from some other regions in ATL: temporal pole (TGd) and MTG (TE1a). These sites were closer to auditory than visual cortex, and were largely overlapping with the limbic network, as opposed to DMN. Both of these sites deactivated to visual feature matching and TE1a (MTG) was consistently deactivated across both Studies 1 and 2, while TGd only showed activation during emotion generation. Both sites also differed from all other ATL regions, including TGv, in not showing preferential activation to the generate versus the switch phase of Study 1. These sites are activated by theory of mind tasks (Balgova et al., 2022; Binney et al., 2016) and therefore might be more strongly recruited for tasks that require greater self and social semantic processing than the tasks employed in the current investigation. The stronger response to emotion than contexts in the temporal pole also fits well with the proposal by the graded hub-and-spoke model

that valence inputs merge into the heteromodal hub via temporopolar connections (Matthew A. Lambon Ralph et al., 2017).

Persichetti et al. (2021) noted that the regions in their parcellation could be readily separated in terms of their intrinsic connectivity patterns when pairs of parcels were compared, which led them to favour a patchwork organisation. However, this finding is also compatible with our macroscale gradient, which not only predicts that there should be differences between regions but also anticipates that the magnitude of these differences will depend on which parcels are compared. Indeed, other parcellations of the ATL which did not prespecify a hard or smooth separation between regions provide further evidence for a gradient in the temporal lobe: task-based and resting-state data show graded transitions from posterior (superior and inferior) unimodal to heteromodal processing in ventral ATL (Bajada et al., 2017; Rebecca L. Jackson et al., 2018). Thus, graded transitions may underlie the separation of the ATL into relatively distinct regions, when hard shifts are stipulated by the parcellation methods used. Indeed, there is alignment between prior hard parcellations (Persichetti et al., 2021) and the dimensional transitions (Rebecca L. Jackson et al., 2018) which could underpin them. Recent work has focussed on how patterns of functional change within the temporal lobe relate to whole-brain connectivity gradients, which capture gradual and systematic changes in intrinsic connectivity across the cortical surface (Margulies et al., 2016; Wang, Margulies, Smallwood, & Jefferies, 2020). The principal gradient in whole-brain decompositions of resting-state fMRI captures the difference in connectivity between unimodal and heteromodal cortex, with the heteromodal end of this dimension associated with abstract, memory-based representations, including in ATL (Murphy et al., 2018; Murphy et al., 2019). In this way, the whole-brain principal gradient aligns well with many of our results. Nevertheless, our focus on large regions of interest and a macroscale gradient does not permit an investigation of whether there is a patchwork functional organisation in this region of cortex at a finer spatial scale. We are also unable to test the smoothness of functional transitions across the ATL's surface, although we do show systematic changes in functional responses across parcels.

By leveraging different semantic content (associative, feature, emotion, context) and tasks (matching, generative), we were able to investigate functional transitions along the ATL, demonstrating a graded response influenced by proximity to spoke regions. This was particularly clear at the auditory end of the gradient, where there was preferential activation for global associations over feature decisions and for the generation of emotion versus context associations. In line with the graded hub perspective, the response profile becomes more equal across semantic content types in more anterior and ventral parcels sandwiched between regions closest to auditory and visual inputs.

Funding: The study was funded by the European Research Council [FLEXSEM-771863], and by the Scientific Foundation of Institute of Psychology, Chinese Academy of Sciences (Grant No. E1CX4725CX; Grant No. E2CX3625CX) to X.W.

References

Bajada, C. J., Jackson, R. L., Haroon, H. A., Azadbakht, H., Parker, G. J. M., Lambon Ralph, M. A., et al. (2017). A graded tractographic parcellation of the temporal lobe. *NeuroImage,* 155, 503-512.

Balgova, E., Diveica, V., Walbrin, J., & Binney, R. J. (2022). The role of the ventrolateral anterior temporal lobes in social cognition. *Human Brain Mapping,* 43(15), 4589-4608.

Barch, D. M., Burgess, G. C., Harms, M. P., Petersen, S. E., Schlaggar, B. L., Corbetta, M., et al. (2013). Function in the human connectome: Task-fMRI and individual differences in behavior. *NeuroImage,* 80, 169-189.

Binney, R. J., Embleton, K. V., Jefferies, E., Parker, G. J. M., & Lambon Ralph, M. A. (2010). The Ventral and Inferolateral Aspects of the Anterior Temporal Lobe Are Crucial in Semantic Memory: Evidence from a Novel Direct Comparison of Distortion-Corrected fMRI, rTMS, and Semantic Dementia. *Cerebral Cortex,* 20(11), 2728-2738.

Binney, R. J., Hoffman, P., & Lambon Ralph, M. A. (2016). Mapping the Multiple Graded Contributions of the Anterior Temporal Lobe Representational Hub to Abstract and Social Concepts: Evidence from Distortion-corrected fMRI. *Cerebral Cortex,* 26(11), 4227-4241.

Borghesani, V., Narvid, J., Battistella, G., Shwe, W., Watson, C., Binney, R. J., et al. (2019). "Looks familiar, but I do not know who she is": The role of the anterior right temporal lobe in famous face recognition. *Cortex,* 115, 72-85.

Chen, Y., Shimotake, A., Matsumoto, R., Kunieda, T., Kikuchi, T., Miyamoto, S., et al. (2016). The 'when' and 'where' of semantic coding in the anterior temporal lobe: Temporal representational similarity analysis of electrocorticogram data. *Cortex,* 79, 1-13.

Coutanche, M. N., & Thompson-Schill, S. L. (2014). Creating Concepts from Converging Features in Human Cortex. *Cerebral Cortex,* 25(9), 2584-2593.

Dale, A. M. (1999). Optimal experimental design for event-related fMRI. *Human brain mapping,* 8(1065-9471 (Print)), 5.

Damasio, H., Tranel D Fau - Grabowski, T., Grabowski T Fau - Adolphs, R., Adolphs R Fau - Damasio, A., & Damasio, A. (2004). Neural systems behind word and concept retrieval. (0010-0277 (Print)).

Duncan, J. (2010). The multiple-demand (MD) system of the primate brain: mental programs for intelligent behaviour. *Trends in Cognitive Sciences,* 14(4), 172-179.

Embleton, K. V., Haroon, H. A., Morris, D. M., Ralph, M. A. L., & Parker, G. J. M. (2010). Distortion correction for diffusion-weighted MRI tractography and fMRI in the temporal lobes. *Human Brain Mapping,* 31(10), 1570-1587.

Fedorenko, E., Duncan, J., & Kanwisher, N. (2013). Broad domain generality in focal regions of frontal and parietal cortex. *Proc Natl Acad Sci U S A,* 110(41), 16616-16621.

Fischl, B., Sereno, M. I., & Dale, A. M. (1999). Cortical Surface-Based Analysis: II: Inflation, Flattening, and a Surface-Based Coordinate System. *NeuroImage,* 9(2), 195-207.

Gainotti, G. (2015). Is the difference between right and left ATLs due to the distinction between general and social cognition or between verbal and non-verbal representations? *Neuroscience & Biobehavioral Reviews,* 51, 296-312.

Glasser, M. F., Coalson, T. S., Robinson, E. C., Hacker, C. D., Harwell, J., Yacoub, E., et al. (2016). A multi-modal parcellation of human cerebral cortex. *Nature,* 536(7615), 171-178.

Glasser, M. F., Sotiropoulos, S. N., Wilson, J. A., Coalson, T. S., Fischl, B., Andersson, J. L., et al. (2013). The minimal preprocessing pipelines for the Human Connectome Project. *NeuroImage,* 80, 105-124.

Gonzalez Alam, T. R. d. J., McKeown, B. L. A., Gao, Z., Bernhardt, B., Vos de Wael, R., Margulies, D. S., et al. (2022). A tale of two gradients: differences between the left and right hemispheres predict semantic cognition. *Brain Structure and Function,* 227(2), 631-654.

Gonzalez Alam, T. R. J., Karapanagiotidis, T., Smallwood, J., & Jefferies, E. (2019). Degrees of lateralisation in semantic cognition: Evidence from intrinsic connectivity. *NeuroImage*, 116089.

Halai, A. D., Parkes, L. M., & Welbourne, S. R. (2015). Dual-echo fMRI can detect activations in inferior temporal lobe during intelligible speech comprehension. *NeuroImage,* 122, 214-221.

Halai, A. D., Welbourne, S. R., Embleton, K., & Parkes, L. M. (2014). A comparison of dual gradient-echo and spin-echo fMRI of the inferior temporal lobe. *Human Brain Mapping,* 35(8), 4118-4128.
Hoenig, K., Sim Ej Fau - Bochev, V., Bochev V Fau - Herrnberger, B., Herrnberger B Fau - Kiefer, M., & Kiefer, M. (2008). Conceptual flexibility in the human brain: dynamic recruitment of semantic maps from visual, motor, and motion-related areas. (0898-929X (Print)).
Huang, C. C., Rolls, E. A.-O., Feng, J., & Lin, C. P. (2022). An extended Human Connectome Project multimodal parcellation atlas of the human cortex and subcortical areas. *Brain structure & function,* 227(3)(1863-2661 (Electronic)), 763–778.
Humphreys, G. F., Hoffman, P., Visser, M., Binney, R. J., & Lambon Ralph, M. A. (2015). Establishing task- and modality-dependent dissociations between the semantic and default mode networks. *Proceedings of the National Academy of Sciences of the United States of America,* 112(25), 7857-7862.
Irish, M., Hodges, J. R., & Piguet, O. (2014). Right anterior temporal lobe dysfunction underlies theory of mind impairments in semantic dementia. *Brain,* 137(4), 1241-1253.
Jackson, R. L. (2021). The neural correlates of semantic control revisited. *NeuroImage,* 224, 117444.
Jackson, R. L., Bajada, C. J., Rice, G. E., Cloutman, L. L., & Lambon Ralph, M. A. (2018). An emergent functional parcellation of the temporal cortex. *NeuroImage,* 170, 385-399.
Jackson, R. L., Hoffman, P., Pobric, G., & Lambon Ralph, M. A. (2015). The Nature and Neural Correlates of Semantic Association versus Conceptual Similarity. *Cerebral Cortex,* 25(11), 4319-4333.
Jackson, R. L., Hoffman, P., Pobric, G., & Lambon Ralph, M. A. (2016). The Semantic Network at Work and Rest: Differential Connectivity of Anterior Temporal Lobe Subregions. *J Neurosci,* 36(5), 1490-1501.
Jefferies, E., & Lambon Ralph, M. A. (2006). Semantic impairment in stroke aphasia versus semantic dementia: a case-series comparison. *Brain,* 129(Pt 8), 2132-2147.
Jenkinson, M., Bannister, P., Brady, M., & Smith, S. (2002). Improved Optimization for the Robust and Accurate Linear Registration and Motion Correction of Brain Images. *Neuroimage,* 17(2), 825-841.
Jenkinson, M., & Smith, S. (2001). A global optimisation method for robust affine registration of brain images. *Medical Image Analysis,* 5(2), 143-156.
Kundu, P., Brenowitz, N. D., Voon, V., Worbe, Y., Vértes, P. E., Inati, S. J., et al. (2013). Integrated strategy for improving functional connectivity mapping using multiecho fMRI. *Proceedings of the National Academy of Sciences,* 110(40), 16187.
Kundu, P., Inati Sj Fau - Evans, J. W., Evans Jw Fau - Luh, W.-M., Luh Wm Fau - Bandettini, P. A., & Bandettini, P. A. (2012). Differentiating BOLD and non-BOLD signals in fMRI time series using multi-echo EPI. (1095-9572 (Electronic)).
Lambon Ralph, M. A. (2014). Neurocognitive insights on conceptual knowledge and its breakdown. (1471-2970 (Electronic)).
Lambon Ralph, M. A., Cipolotti, L., Manes, F., & Patterson, K. (2010). Taking both sides: do unilateral anterior temporal lobe lesions disrupt semantic memory? *Brain,* 133(11), 3243-3255.
Lambon Ralph, M. A., Ehsan, S., Baker, G. A., & Rogers, T. T. (2012). Semantic memory is impaired in patients with unilateral anterior temporal lobe resection for temporal lobe epilepsy. *Brain : a journal of neurology,* 135(Pt 1), 242-258.
Lambon Ralph, M. A., Jefferies, E., Patterson, K., & Rogers, T. T. (2017). The neural and computational bases of semantic cognition. *Nature Reviews Neuroscience,* 18, 42.
Lambon Ralph, M. A., Lowe, C., & Rogers, T. T. (2007). Neural basis of category-specific semantic deficits for living things: evidence from semantic dementia, HSVE and a neural network model. *Brain,* 130(4), 1127-1137.
Lambon Ralph, M. A., Sage, K., Jones, R. W., & Mayberry, E. J. (2010). Coherent concepts are computed in the anterior temporal lobes. *Proceedings of the National Academy of Sciences,* 107(6), 2717-2722.

Lang, P. J., Brady, M. M., & Cuthbert, B. N. (2008). International affective picture system (IAPS): Affective ratings of pictures and instruction manual.
Margulies, D. S., Ghosh, S. S., Goulas, A., Falkiewicz, M., Huntenburg, J. M., Langs, G., et al. (2016). Situating the default-mode network along a principal gradient of macroscale cortical organization. *Proceedings of the National Academy of Sciences,* 113(44), 12574.
Martin, A. (2007). The representation of object concepts in the brain. *Annual Review of Psychology,* 58, 25-45.
Mitchell, J. S. B., Mount, D. M., & Papadimitriou, C. H. (1987). The Discrete Geodesic Problem. *SIAM Journal on Computing,* 16(4), 647-668.
Murphy, C., Jefferies, E., Rueschemeyer, S.-A., Sormaz, M., Wang, H.-t., Margulies, D. S., et al. (2018). Distant from input: Evidence of regions within the default mode network supporting perceptually-decoupled and conceptually-guided cognition. *NeuroImage,* 171, 393-401.
Murphy, C., Rueschemeyer, S.-A., Watson, D., Karapanagiotidis, T., Smallwood, J., & Jefferies, E. (2017). Fractionating the anterior temporal lobe: MVPA reveals differential responses to input and conceptual modality. *NeuroImage,* 147, 19-31.
Murphy, C., Wang, H.-T., Konu, D., Lowndes, R., Margulies, D. S., Jefferies, E., et al. (2019). Modes of operation: A topographic neural gradient supporting stimulus dependent and independent cognition. *NeuroImage,* 186, 487-496.
Noppeney, U., Patterson, K., Tyler, L. K., Moss, H., Stamatakis, E. A., Bright, P., et al. (2007). Temporal lobe lesions and semantic impairment: a comparison of herpes simplex virus encephalitis and semantic dementia. *Brain,* 130(4), 1138-1147.
O'Rourke, J. (1999). Computational geometry column 35. *SIGACT News,* 30(2), 31–32.
Olson, I. R., McCoy, D., Klobusicky, E., & Ross, L. A. (2013). Social cognition and the anterior temporal lobes: a review and theoretical framework. *Social Cognitive and Affective Neuroscience,* 8(2), 123-133.
Olson, I. R., Plotzker A Fau - Ezzyat, Y., & Ezzyat, Y. (2007). The Enigmatic temporal pole: a review of findings on social and emotional processing. (1460-2156 (Electronic)).
Patterson, K., Nestor, P. J., & Rogers, T. T. (2007). Where do you know what you know? The representation of semantic knowledge in the human brain. *Nat Rev Neurosci,* 8(12), 976-987.
Persichetti, A. S., Denning, J. M., Gotts, S. J., & Martin, A. (2021). A Data-Driven Functional Mapping of the Anterior Temporal Lobes. *The Journal of Neuroscience,* 41(28), 6038.
Poser, B. A., & Norris, D. G. (2007). Fast spin echo sequences for BOLD functional MRI. *Magnetic Resonance Materials in Physics, Biology and Medicine,* 20(1), 11-17.
Poser, B. A., Versluis, M. J., Hoogduin, J. M., & Norris, D. G. (2006). BOLD contrast sensitivity enhancement and artifact reduction with multiecho EPI: Parallel-acquired inhomogeneity-desensitized fMRI. *Magnetic Resonance in Medicine,* 55(6), 1227-1235.
Rice, G. E., Caswell, H., Moore, P., Hoffman, P., & Lambon Ralph, M. A. (2018). The Roles of Left Versus Right Anterior Temporal Lobes in Semantic Memory: A Neuropsychological Comparison of Postsurgical Temporal Lobe Epilepsy Patients. *Cerebral Cortex,* 28(4), 1487-1501.
Rice, G. E., Hoffman, P., Binney, R. J., & Lambon Ralph, M. A. (2018). Concrete versus abstract forms of social concept: an fMRI comparison of knowledge about people versus social terms. *Philosophical Transactions of the Royal Society B: Biological Sciences,* 373(1752), 20170136.
Rice, G. E., Hoffman, P., & Lambon Ralph, M. A. (2015). Graded specialization within and between the anterior temporal lobes. *Annals of the New York Academy of Sciences,* 1359(1), 84-97.
Rice, G. E., Lambon Ralph, M. A., & Hoffman, P. (2015). The Roles of Left Versus Right Anterior Temporal Lobes in Conceptual Knowledge: An ALE Meta-analysis of 97 Functional Neuroimaging Studies. *Cerebral Cortex,* 25(11), 4374-4391.
Robinson, E. C., Jbabdi, S., Glasser, M. F., Andersson, J., Burgess, G. C., Harms, M. P., et al. (2014). MSM: A new flexible framework for Multimodal Surface Matching. *NeuroImage,* 100, 414-426.

Rogers, T. T., Cox, C. R., Lu, Q., Shimotake, A., Kikuchi, T., Kunieda, T., et al. (2021). Evidence for a deep, distributed and dynamic code for animacy in human ventral anterior temporal cortex. *eLife,* 10, e66276.
Schapiro, A. C., McClelland, J. L., Welbourne, S. R., Rogers, T. T., & Lambon Ralph, M. A. (2013). Why Bilateral Damage Is Worse than Unilateral Damage to the Brain. *Journal of Cognitive Neuroscience,* 25(12), 2107-2123.
Simmons, W. K., Martin A Fau - Barsalou, L. W., & Barsalou, L. W. (2005). Pictures of appetizing foods activate gustatory cortices for taste and reward. (1047-3211 (Print)).
Smith, S. M., Jenkinson, M., Woolrich, M. W., Beckmann, C. F., Behrens, T. E. J., Johansen-Berg, H., et al. (2004). Advances in functional and structural MR image analysis and implementation as FSL. *NeuroImage,* 23, S208-S219.
Van Essen, D. C., Donahue, C. J., Coalson, T. S., Kennedy, H., Hayashi , T., & Glasser, M. F. (2019). Cerebral cortical folding, parcellation, and connectivity in humans, nonhuman primates, and mice. . *PNAS,* 116(52), 7.
Visser, M., Embleton, K. V., Jefferies, E., Parker, G. J., & Ralph, M. A. L. (2010). The inferior, anterior temporal lobes and semantic memory clarified: Novel evidence from distortion-corrected fMRI. *Neuropsychologia,* 48(6), 1689-1696.
Visser, M., Jefferies, E., Embleton, K. V., & Lambon Ralph, M. A. (2012). Both the Middle Temporal Gyrus and the Ventral Anterior Temporal Area Are Crucial for Multimodal Semantic Processing: Distortion-corrected fMRI Evidence for a Double Gradient of Information Convergence in the Temporal Lobes. *Journal of Cognitive Neuroscience,* 24(8), 1766-1778.
Visser, M., Jefferies, E., & Lambon Ralph, M. A. (2009). Semantic Processing in the Anterior Temporal Lobes: A Meta-analysis of the Functional Neuroimaging Literature. *Journal of Cognitive Neuroscience,* 22(6), 1083-1094.
Visser, M., & Lambon Ralph, M. A. (2011). Differential contributions of bilateral ventral anterior temporal lobe and left anterior superior temporal gyrus to semantic processes. *J Cogn Neurosci,* 23(10), 3121-3131.
Wang, X., Krieger-Redwood, K., Zhang, M., Cui, Z., Wang, X., Karapanagiotidis, T., et al. (2023). Physical distance to sensory-motor landmarks predicts language function. *Cerebral Cortex,* 33(8), 4305-4318.
Wang, X., Margulies, D. S., Smallwood, J., & Jefferies, E. (2020). A gradient from long-term memory to novel cognition: Transitions through default mode and executive cortex. *NeuroImage,* 220, 117074.
Woolrich, M. W., Jbabdi, S., Patenaude, B., Chappell, M., Makni, S., Behrens, T., et al. (2009). Bayesian analysis of neuroimaging data in FSL. *NeuroImage,* 45(1, Supplement 1), S173-S186.
Woolrich, M. W., Ripley, B. D., Brady, M., & Smith, S. M. (2001). Temporal Autocorrelation in Univariate Linear Modeling of FMRI Data. *NeuroImage,* 14(6), 1370-1386.
Yeo, B. T., Krienen, F. M., Sepulcre, J., Sabuncu, M. R., Lashkari, D., Hollinshead, M., et al. (2011). The organization of the human cerebral cortex estimated by intrinsic functional connectivity. *J Neurophysiol,* 106(3), 1125-1165.
Zahn, R., Moll J Fau - Krueger, F., Krueger F Fau - Huey, E. D., Huey Ed Fau - Garrido, G., Garrido G Fau - Grafman, J., & Grafman, J. (2007). Social concepts are represented in the superior anterior temporal cortex. (0027-8424 (Print)).

Supplementary Materials

ID	Description	Valence Mean	Valence SD	Arousal Mean	Arousal SD	Association Type	Valence
1120	Snake	3.79	1.93	6.93	1.68	Emotion	Neg
1350	Pig	5.25	1.96	4.37	1.76	Semantic Context	Neut
1390	Bees	4.5	1.56	5.29	1.97	Semantic Context	Neut
1659	Gorilla	6.57	1.98	4.89	1.97	Emotion	Pos
1675	Buffalo	5.24	1.48	4.37	2.15	Semantic Context	Neut
1999	Mickey	7.43	1.47	4.77	2.4	Emotion	Pos
2002	Man	4.95	1.36	3.35	1.87	Semantic Context	Neut
2036	Woman	5.8	1.28	3.24	1.88	Semantic Context	Neut
2039	Woman	3.65	1.44	3.46	1.94	Emotion	Neg
2092	Clowns	6.28	1.9	4.32	2.29	Emotion	Pos
2156	Family	7.12	1.46	4.34	2.11	Emotion	Pos
2191	Farmer	5.3	1.62	3.61	2.14	Semantic Context	Neut
2217	Class	6.24	1.52	4.08	1.85	Emotion	Pos
2360	Family	7.7	1.76	3.66	2.32	Emotion	Pos
2377	Reading	5.19	1.31	3.5	1.95	Semantic Context	Neut
2382	Artist	5.67	1.19	3.75	1.97	Semantic Context	Neut
2383	Secretary	4.72	1.36	3.41	1.83	Semantic Context	Neut
2390	Couple	5.4	1.18	3.57	1.92	Semantic Context	Neut
2397	Men	4.98	1.11	2.77	1.74	Semantic Context	Neut
2455	SadGirls	2.96	1.79	4.46	2.12	Emotion	Neg
2456	CryingFamily	2.84	1.27	4.55	2.16	Emotion	Neg
2488	Musician	5.73	1.14	3.91	1.87	Semantic Context	Neut
2489	Musician	5.66	1.44	3.8	1.93	Semantic Context	Neut
2490	Man	3.32	1.82	3.95	2	Emotion	Neg
2595	Women	4.88	1.24	3.71	1.88	Semantic Context	Neut
2635	Cowboy	5.22	1.65	4.42	1.98	Semantic Context	Neut
2691	Riot	3.04	1.73	5.85	2.03	Emotion	Neg
2718	DrugAddict	3.65	1.58	4.46	2.03	Emotion	Neg
2745.1	Shopping	5.31	1.08	3.26	1.96	Semantic Context	Neut
2751	DrunkDriving	2.67	1.87	5.18	2.39	Emotion	Neg
2870	Teenager	5.31	1.41	3.01	1.72	Semantic Context	Neut
2980	FoodBasket	5.61	1.5	3.09	1.91	Semantic Context	Neut
5300	Galaxy	6.91	1.8	4.36	2.62	Emotion	Pos
5455	Cockpit	5.79	1.37	4.56	2.17	Semantic Context	Neut
5500	Mushroom	5.42	1.58	3	2.42	Semantic Context	Neut
5621	SkyDivers	7.57	1.42	6.99	1.95	Emotion	Pos
5623	Windsurfers	7.19	1.44	5.67	2.32	Emotion	Pos
5814	Mountain	7.15	1.54	4.82	2.4	Emotion	Pos
5900	Desert	5.93	1.64	4.38	2.1	Semantic Context	Neut
5910	Fireworks	7.8	1.23	5.59	2.55	Emotion	Pos
6240	Gun	3.79	1.8	5.27	2.2	Emotion	Neg
7001	Buttons	5.32	1.19	3.2	2.15	Semantic Context	Neut
7033	Train	5.4	1.57	3.99	2.14	Semantic Context	Neut
7036	Shipyard	4.88	1.08	3.32	2.04	Semantic Context	Neut
7081	Luggage	5.36	1.3	3.96	2.24	Semantic Context	Neut
7130	Truck	4.77	1.03	3.35	1.9	Semantic Context	Neut

7234	IroningBoard	4.23	1.58	2.96	1.9	Semantic Context	Neut
7325	Watermelon	7.06	1.65	3.55	2.07	Emotion	Pos
7492	Ferry	7.41	1.68	4.91	2.46	Emotion	Pos
7493	Man	5.35	1.34	3.39	2.08	Semantic Context	Neut
7495	Store	5.9	1.6	3.82	2.33	Semantic Context	Neut
7496	Street	5.92	1.66	4.84	1.99	Semantic Context	Neut
7503	CardDealer	5.77	1.39	4.21	2.39	Semantic Context	Neut
7506	Casino	5.34	1.46	4.25	1.95	Semantic Context	Neut
7509	Paintbrush	6.03	1.35	3.43	2.02	Emotion	Pos
7520	Hospital	3.83	1.56	4.57	1.85	Emotion	Neg
7530	House	6.71	1.36	4	2.14	Emotion	Pos
7560	Freeway	4.47	1.65	5.24	2.03	Semantic Context	Neut
7710	Bed	5.42	1.58	3.44	2.21	Semantic Context	Neut
8158	Hiker	6.53	1.66	6.49	2.05	Emotion	Pos
8180	CliffDivers	7.12	1.88	6.59	2.12	Emotion	Pos
8312	Golf	5.37	1.41	3.32	2.06	Semantic Context	Neut
8325	RaceCars	5.63	1.5	4.47	2.19	Semantic Context	Neut
8499	Rollercoaster	7.63	1.41	6.07	2.31	Emotion	Pos
9090	Exhaust	3.56	1.5	3.97	2.12	Emotion	Neg
9110	Puddle	3.76	1.41	3.98	2.23	Emotion	Neg
9220	Cemetery	2.06	1.54	4	2.09	Emotion	Neg
9342	Pollution	2.85	1.41	4.49	1.88	Emotion	Neg
9445	Skeleton	3.87	1.57	4.49	2.01	Emotion	Neg
9622	Jet	3.1	1.9	6.26	1.98	Emotion	Neg
9630	Bomb	2.96	1.72	6.06	2.22	Emotion	Neg
9832	Cigarettes	2.94	1.58	4.46	2.06	Emotion	Neg

Supplementary Table S1. Identifiers for stimuli taken from the International Affective Picture System with mean and SD of valence and arousal ratings, and allocation of association type and categorical valence in the current study. Neg = Negative, Neut = Neutral, Pos = Positive.

Reordered ID (L, R)	Region	RegionLongName	Cortical Division	Cortex ID	Original ID	Voxel numbers (1 mm3) (L,R)
62, 242	STGa	Area_STGa	Auditory_Association	11	123	2509, 2187
82, 262	EC	Entorhinal_Cortex	Medial_Temporal	13	118	2127, 2110
83, 263	PeEc	Perirhinal_Ectorhinal_Cortex	Medial_Temporal	13	122	4826, 4755
89, 269	TE1a	Area_TE1_anterior	Lateral_Temporal	14	132	5227, 4180
94, 274	TGd	Area_TG_dorsal	Lateral_Temporal	14	131	10,192, 10,269
95, 275	TGv	Area_TG_Ventral	Lateral_Temporal	14	172	3694, 4515

Supplementary Table S2. Glasser labels and HCPex labels for the regions included in this investigation.

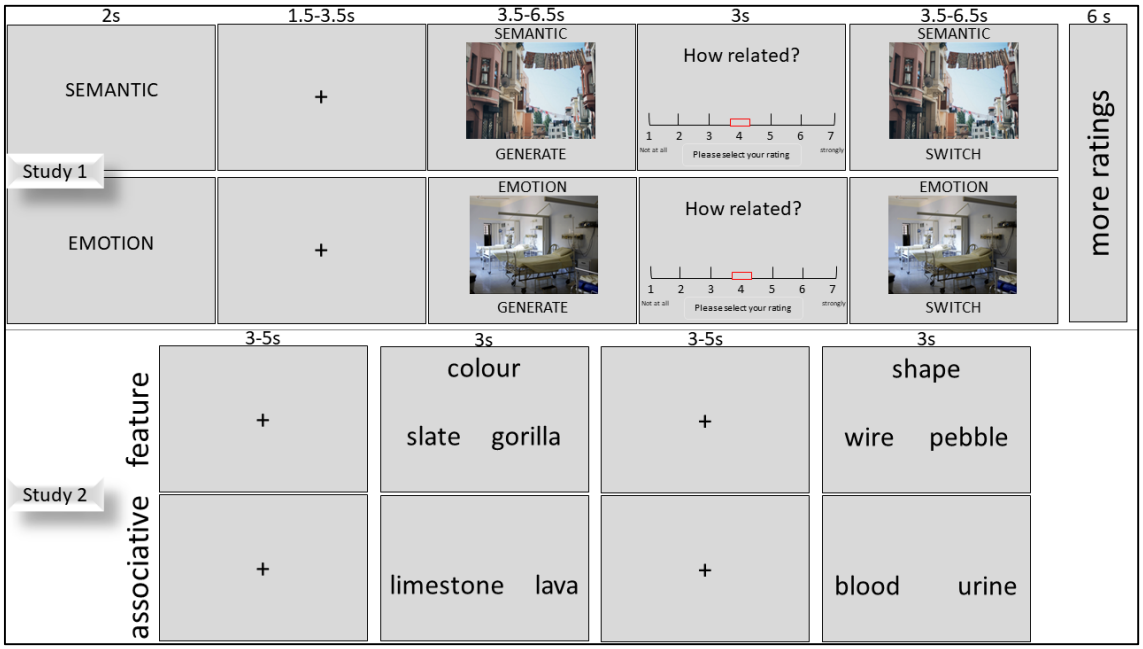

Figure S1: Task schematic for Study 1 (top) and Study 2 (bottom).

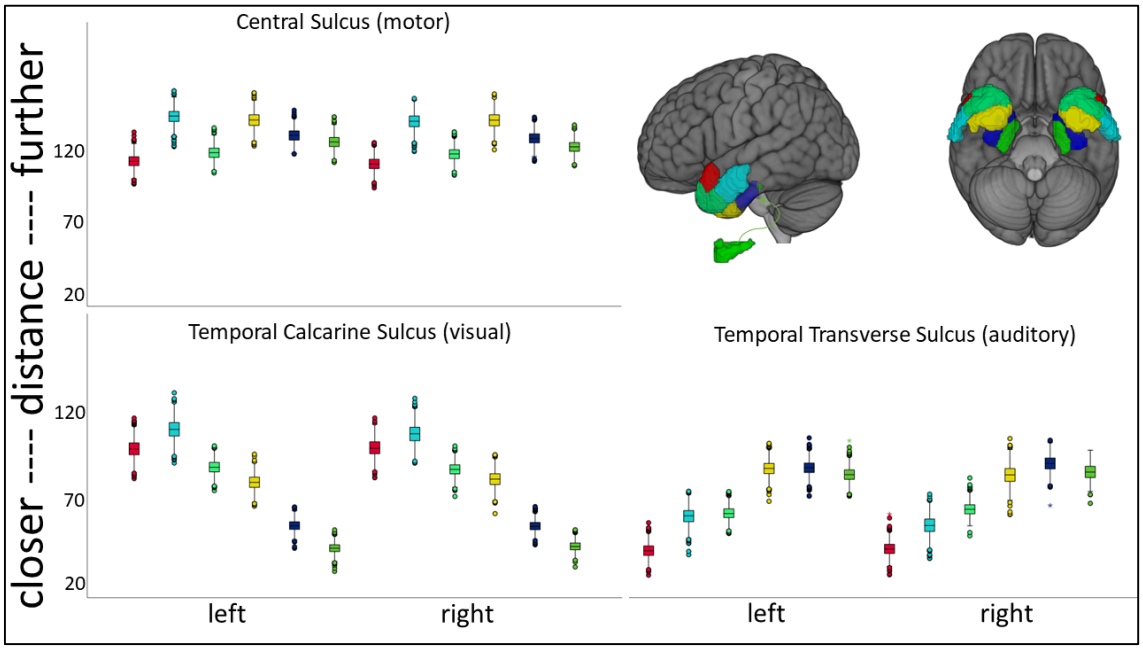

Figure S2: Minimum distance (averaged across all the vertices in each ATL parcel) of ATL parcels to primary sensory-motor regions (motor, visual and auditory). Smaller numbers = closer proximity. The parcels are colour-coded and presented in the following order from left to right: Red = STGa; Cyan = TE1a (MTG); Mint = TGd (temporal pole); Yellow = TGv (aITG/fusiform); Dark blue = PeEc (fusiform); Green = EC (parahippocampal).

Activation in Study 1: Emotion and Semantic Context Generation and Switch

	Sphericity	df	F	*p*
emotion/semantic	Sphericity Assumed	1,31	4.312	**0.046**
generate/switch	Sphericity Assumed	1,31	12.449	**0.001**
left/right	Sphericity Assumed	1,31	20.865	**<.001**
parcel	Greenhouse-Geisser	3, 88	15.495	**<.001**
emotion/semantic * generate/switch	Sphericity Assumed	1,31	0.072	0.79
emotion/semantic * left/right	Sphericity Assumed	1,31	0.946	0.338
generate/switch * left/right	Sphericity Assumed	1,31	0.678	0.416
emotion/semantic * generate/switch * left/right	Sphericity Assumed	1,31	2.394	0.132
emotion/semantic * parcel	Greenhouse-Geisser	3, 91	23.355	**<.001**
generate/switch * parcel	Greenhouse-Geisser	3, 99	10.432	**<.001**
emotion/semantic * generate/switch * parcel	Greenhouse-Geisser	3, 88	2.064	0.114
left/right * parcel	Greenhouse-Geisser	3, 89	12.74	**<.001**
emotion/semantic * left/right * parcel	Greenhouse-Geisser	4, 111	0.495	0.718
generate/switch * left/right * parcel	Greenhouse-Geisser	4, 117	1.889	0.121
emotion/semantic * generate/switch * left/right * parcel	Sphericity Assumed	5,155	1.328	0.255

Table S3. Omnibus ANOVA: Association (emotion/semantic) by Phase (generate/switch) by hemisphere (left/right) by parcel (STGa, TE1a, TGd, TGv, PeEc, EC).

	Sphrecity	df	F	*p*
emotion/semantic	Sphericity Assumed	1, 31	6.06	**0.02**
left/right	Sphericity Assumed	1, 31	2.867	0.1
parcel	Greenhouse-Geisser	2, 74	0.537	0.618
emotion/semantic * left/right	Sphericity Assumed	1, 31	1.107	0.301
emotion/semantic * parcel	Greenhouse-Geisser	3, 95	0.367	0.78
left/right * parcel	Greenhouse-Geisser	4, 113	1.809	0.138
emotion/semantic * left/right * parcel	Greenhouse-Geisser	4, 112	0.516	0.705

Table S4. Omnibus ANOVA of parametric effect of difficulty: Association (emotion/semantic) by hemisphere (left/right) by parcel (STGa, TE1a, TGd, TGv, PeEc, EC).

These parametric EV's included demeaned switch difficulty scores for each trial within a run, calculated separately for semantic and emotion associations. One run for one participant was excluded from the model as all *emotion* trials were rated the same for switch difficulty – resulting in each trial weighted as 0. Self-reported ratings of association strength for the *generate* and *switch* phase were not modelled as they both correlated with ratings of switch difficulty across the sample [*generate*: $r_s(2230) = -.14$, $p < .001$, *switch*: $r_s(2234) = -.53$, $p < .001$].

Activation in Study 2: Association and Feature Judgments

	Sphericity	df	F	*p*
association/feature	Sphericity Assumed	1, 28	6.1	**0.02**
no/yes	Sphericity Assumed	1, 28	1.245	0.274
left/right	Sphericity Assumed	1, 28	4.017	**0.055**
parcel	Greenhouse-Geisser	3, 72	38.855	**<.001**
association/feature * no/yes	Sphericity Assumed	1, 28	0	0.988
association/feature * left/right	Sphericity Assumed	1, 28	0.352	0.558
no/yes * left/right	Sphericity Assumed	1, 28	2.773	0.107
association/feature * no/yes * left/right	Sphericity Assumed	1, 28	1.075	0.309
association/feature * parcel	Greenhouse-Geisser	3, 81	2.699	**0.053**
no/yes * parcel	Greenhouse-Geisser	3, 95	1.545	0.203
association/feature * no/yes * parcel	Greenhouse-Geisser	3, 88	0.919	0.439
left/right * parcel	Greenhouse-Geisser	3, 81	6.332	**<.001**
association/feature * left/right * parcel	Greenhouse-Geisser	3, 87	0.918	0.439
no/yes * left/right * parcel	Greenhouse-Geisser	3, 96	1.165	0.33
association/feature * no/yes * left/right * parcel	Greenhouse-Geisser	4, 104	0.265	0.888

Table S5. Omnibus ANOVA: Association/feature by decision type (yes/no) by hemisphere (left/right) by parcel (STGa, TE1a, TGd, TGv, PeEc, EC).

	Sphrecity	df	F	*p*
association/feature	Sphericity Assumed	1, 28	6.722	**0.015**
no/yes	Sphericity Assumed	1, 28	0.135	0.716
left/right	Sphericity Assumed	1, 28	4.581	**0.041**
parcel	Greenhouse-Geisser	3, 88	2.44	0.067
association/feature * no/yes	Sphericity Assumed	1, 28	3.019	0.093
association/feature * left/right	Sphericity Assumed	1, 28	0.003	0.954
no/yes * left/right	Sphericity Assumed	1, 28	0.41	0.527
association/feature * no/yes * left/right	Sphericity Assumed	1, 28	4.15	**0.051**
association/feature * parcel	Greenhouse-Geisser	3, 72	0.72	0.523
no/yes * parcel	Greenhouse-Geisser	3, 85	0.908	0.442
association/feature * no/yes * parcel	Greenhouse-Geisser	3, 73	0.422	0.709
left/right * parcel	Greenhouse-Geisser	3, 90	1.957	0.122
association/feature * left/right * parcel	Greenhouse-Geisser	4, 100	0.953	0.43
no/yes * left/right * parcel	Greenhouse-Geisser	3, 78	1.569	0.206
association/feature * no/yes * left/right * parcel	Greenhouse-Geisser	3, 80	1.152	0.332

Table S6. Omnibus ANOVA of parametric effect of association and feature strength: Association/feature by decision type (yes/no) by hemisphere (left/right) by parcel (STGa, TE1a, TGd, TGv, PeEc, EC).